A New Type of Plant Virus Causing Striped Chlorosis of Mimosa

E. M. Martin and K. S. Kim

Department of Plant Pathology, University of Arkansas, Fayetteville 72701.
Published with the approval of the Director of the Arkansas Agricultural Experiment Station, Fayetteville.
Accepted for publication 10 December 1986 (submitted for electronic processing).

ABSTRACT

Martin, E. M., and Kim, K. S. 1987. A new type of plant virus causing striped chlorosis of mimosa. Phytopathology 77:935-940.

Rod-shaped virus-like particles (VLPs) approximately 35 × 95 nm were consistently associated with a chlorotic leaf stripe symptom in mimosa leaves and were seed- and graft-transmissible. In thin-section electron microscopy, the particles, which were arranged tightly parallel to each other along their long axes in paracrystalline arrays, were associated with fibrillar and granular viroplasmic inclusions in the cytoplasm of infected cells. The granular inclusions structurally resembled those induced by caulimoviruses, a group of plant viruses containing double-stranded DNA as their genomic material. Bernhard's regressive staining technique suggested that both the VLPs and granular inclusions found in mimosa contained DNA. No plant viruses having the particle morphology of VLPs of mimosa with a DNA genome have been reported previously.

Chlorotic symptoms suggestive of virus infection were first noted on leaves of a mimosa tree, *Albizzia julibrissin* Durazzini, in northwest Arkansas. The symptoms included intermittent chlorotic stripes parallel to or along major and minor veins of the leaves and diffusing into interveinal regions (Fig. 1). Seedlings grown in the greenhouse from the seeds collected from this tree displayed similar leaf symptoms. The symptoms have recurred in these seedlings and in the original tree for five consecutive years. Preliminary electron microscopic observations indicated that short, rod-shaped, virus-like particles (VLPs) and viroplasmic inclusions were consistently associated with the chlorotic leaf symptoms, suggesting the viral nature of the particles. The structure of the particles and associated inclusions appeared to be distinct from those of other groups of known plant viruses. One of the two types of viroplasmic inclusions, however, resembled the caulimovirus-induced viroplasm. Transmission of the VLPs and the associated cytopathic effects in leaf cells of mimosa trees are reported in this paper.

MATERIALS AND METHODS

Transmission procedures. To test mechanical transmission of the mimosa VLPs, 28 test species from eight families were inoculated. Of the 28 species tested, seven species were Leguminosae, two of which were in the Mimosoideae subfamily. Inocula were either mimosa leaves showing chlorotic symptoms or flowers from these plants ground with mortar and pestle in 0.01 M phosphate buffer, pH 7.0, alone or containing either 0.01 M cysteine hydrochloride, 2.5% nicotine, or 1% 2-mercaptoethanol. The test species were grown from seed sown in steamed soil.

Several grafting methods including bud, cambium, twig, and bark grafts were used to attempt transmission to healthy mimosa test plants grown from seed obtained from Herbst Brothers Seedsmen, Inc., Brewster, NY. Additionally, approach grafts were made from mimosa seedlings with typical leaf symptoms to mimosa seedlings grown from healthy stock.

To test for seed transmissibility, 20 seeds per planting collected from the infected tree were germinated in steamed soil and grown in the greenhouse. This study was carried out over a 2-yr period with three plantings per year.

Electron microscopy. Leaf specimens approximately 2 mm^2 were taken from chlorotic and green areas of mimosa leaves of the originally infected tree, from greenhouse-grown seedlings as young as 2 mo, and from grafted mimosa seedlings, all of which were showing the typical leaf symptoms. Root specimens approximately 2 mm long and 1 mm in diameter were taken from small lateral roots of seedlings with leaf symptoms. Control leaf and root specimens were taken from greenhouse-grown seedlings grown from the healthy stock. Specimens were fixed in a modified Karnovsky's fixative (7) containing 2% paraformaldehyde and 2.5% glutaraldehyde in 0.05 M cacodylate buffer, pH 7.2, and post-fixed in 1% osmium tetroxide in the same buffer. Tissues were bulk-stained overnight in 0.5% aqueous uranyl acetate, dehydrated through an ethanol series, and embedded in Spurr's medium (21).

Thin sections were cut with a diamond knife and stained with 2% aqueous uranyl acetate and lead citrate. Grids were viewed with either a JEM 100 CX or a Siemens IA electron microscope.

To determine whether VLPs and associated inclusions observed in this study were composed of deoxyribonucleoprotein or ribonucleoprotein, Bernhard's uranyl-EDTA-lead staining method (1) was employed. The method has been successfully used for similar studies in both animal (1,20) and plant cells (8,12) infected with either DNA or RNA viruses. For this method, specimens were prepared as described previously (8,12). Also, an alternate

Fig. 1. Two mimosa leaves showing typical chlorotic stripe symptoms.

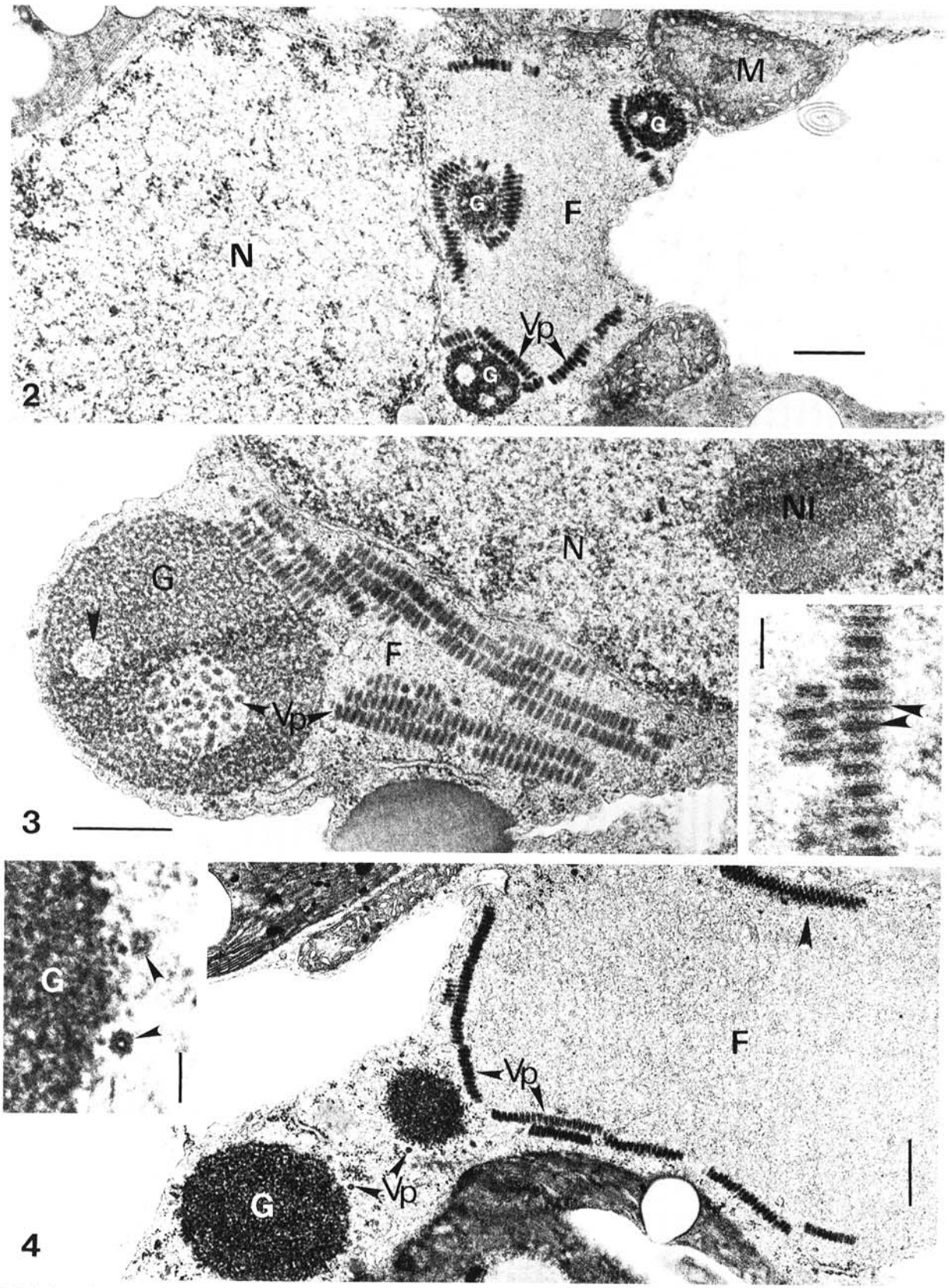

Figs. 2–4. Cells from fully grown mimosa leaves containing virus-like particles (VLPs) and associated granular and fibrillar inclusion bodies. **2,** Portion of a mesophyll cell containing VLPs associated with granular (G) and fibrillar (F) inclusions in the cytoplasm adjacent to the nucleus (N). Virus-like particles (Vp) are seen either in longitudinal, transverse, or oblique sections. M = mitochondria. Bar represents 500 nm. **3,** A large granular inclusion (G) containing two vacuoles. The large vacuole contains randomly arranged VLPs (Vp), whereas the small one (arrowhead) is filled with the material similar to that of the fibrillar inclusions (F). Many layers of VLPs, arranged tightly with their long axes parallel to one another, are embedded in the fibrillar inclusion between the nucleus (N) and a granular inclusion. Nl = nucleolus. Bar represents 500 nm. Inset: A higher magnification of layers of VLPs sectioned longitudinally. Each particle appears as a short rod with an electron-lucent canal (arrowheads). Bar represents 100 nm. **4,** A large fibrillar inclusion (F) bordered by VLP "brick walls" (Vp). Two granular inclusions (G) away from the fibrillar inclusion with VLPs occurring singly (arrowheads) around their periphery are also shown. The particles in one of the VLP "brick layers" (arrowhead) are sectioned in such a way that they exhibit a zig-zag pattern. Bar represents 500 nm. Inset: A higher magnification of a portion of a granular inclusion associated with two transversely sectioned VLPs (arrowheads). Bar represents 100 nm.

method was used for distinguishing between DNA- and RNA-containing structures in aldehyde + osmium fixed specimens (4).

RESULTS

Transmission studies. Several weeks after sap-inoculation using leaves or flowers, none of the 28 species of test plants showed any symptoms suggestive of viral infection. However, in graft experiments between healthy and diseased mimosa, four out of five approach grafted plants showed typical leaf symptoms after 4 mo. No transmission occurred by any other type of grafting.

Twenty-five out of the 120 seedlings grown from seeds collected from the symptom-bearing tree developed similar leaf symptoms within 2–4 mo.

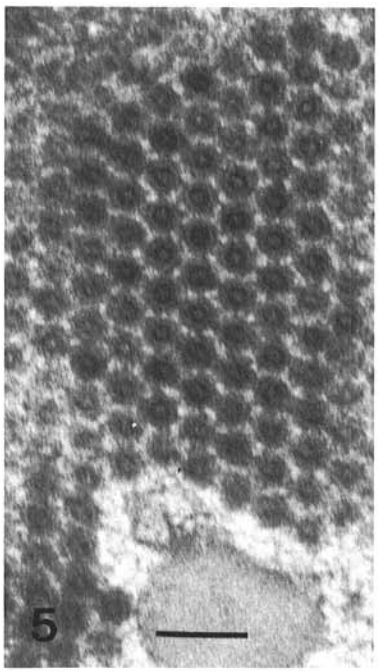

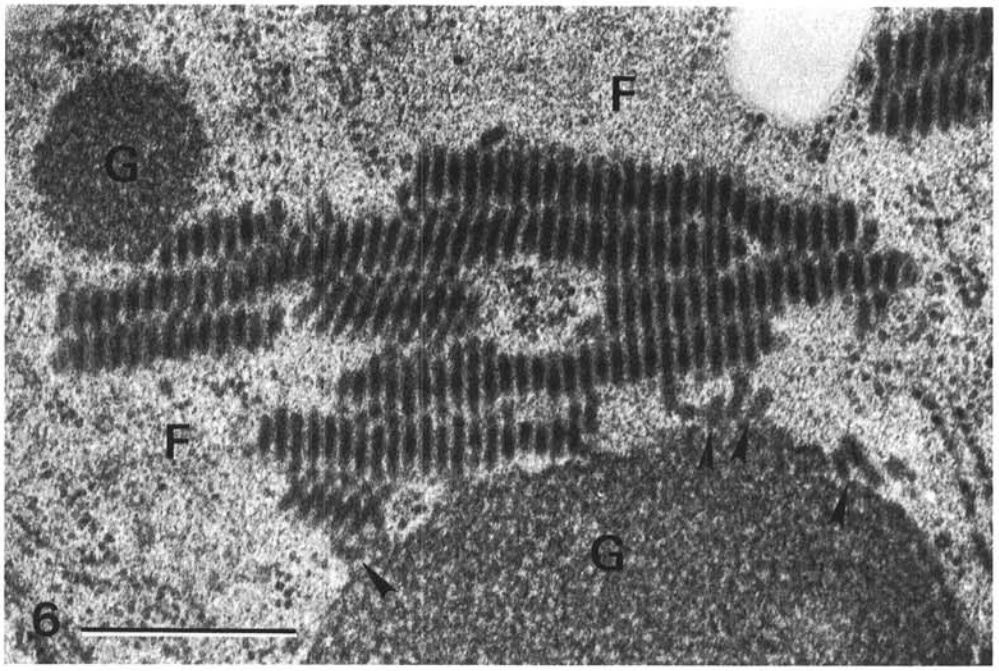

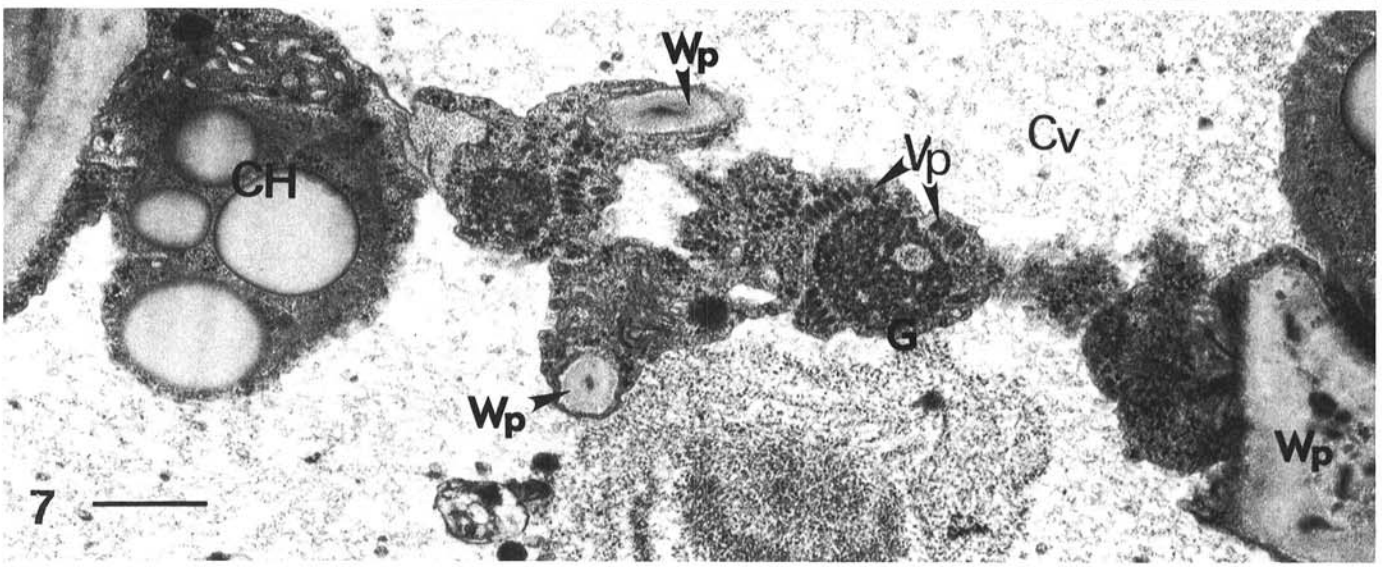

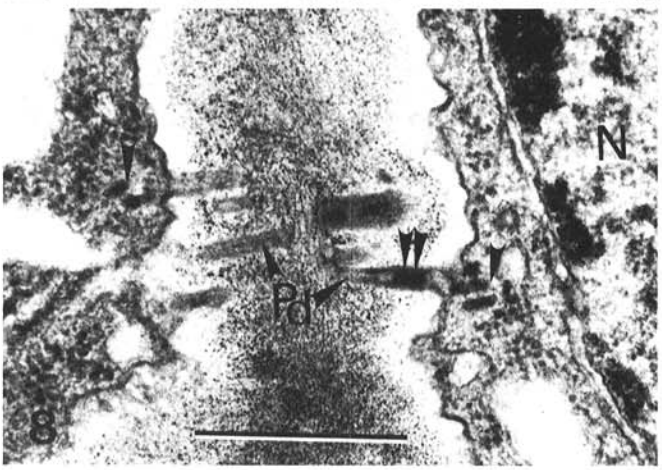

Figs. 5–8. Virus-like particles (VLPs) and associated cytopathic effects found in mimosa leaf mesophyll cells. **5,** Transverse sections of VLP layers that appear as regularly spaced paracrystalline arrays of spheres. Each particle consists of a less electron dense outer coat, and electron-lucent central core, and an electron-dense band between the two. Bar represents 100 nm. **6,** A portion of a large granular inclusion (G) intimately associated with many layers of VLPs. The particles closest to the inclusion appear to be formed by budding (arrowheads) from the granular material. Bar represents 500 nm. **7,** Portion of a leaf cell containing cell wall protuberances (Wp), VLPs (Vp), and granular (G) inclusions. Wall protuberances penetrated deeply into the central vacuole (Cv). When such protuberances were sectioned transversely, they appear as circular profiles as shown in this figure surrounded by the cytoplasm. CH = chloroplast. Bar represents 500 nm. **8,** Virus-like particles occurring near (single arrowheads) and in (double arrowheads) the plasmodesmata (Pd). Bar represents 500 nm.

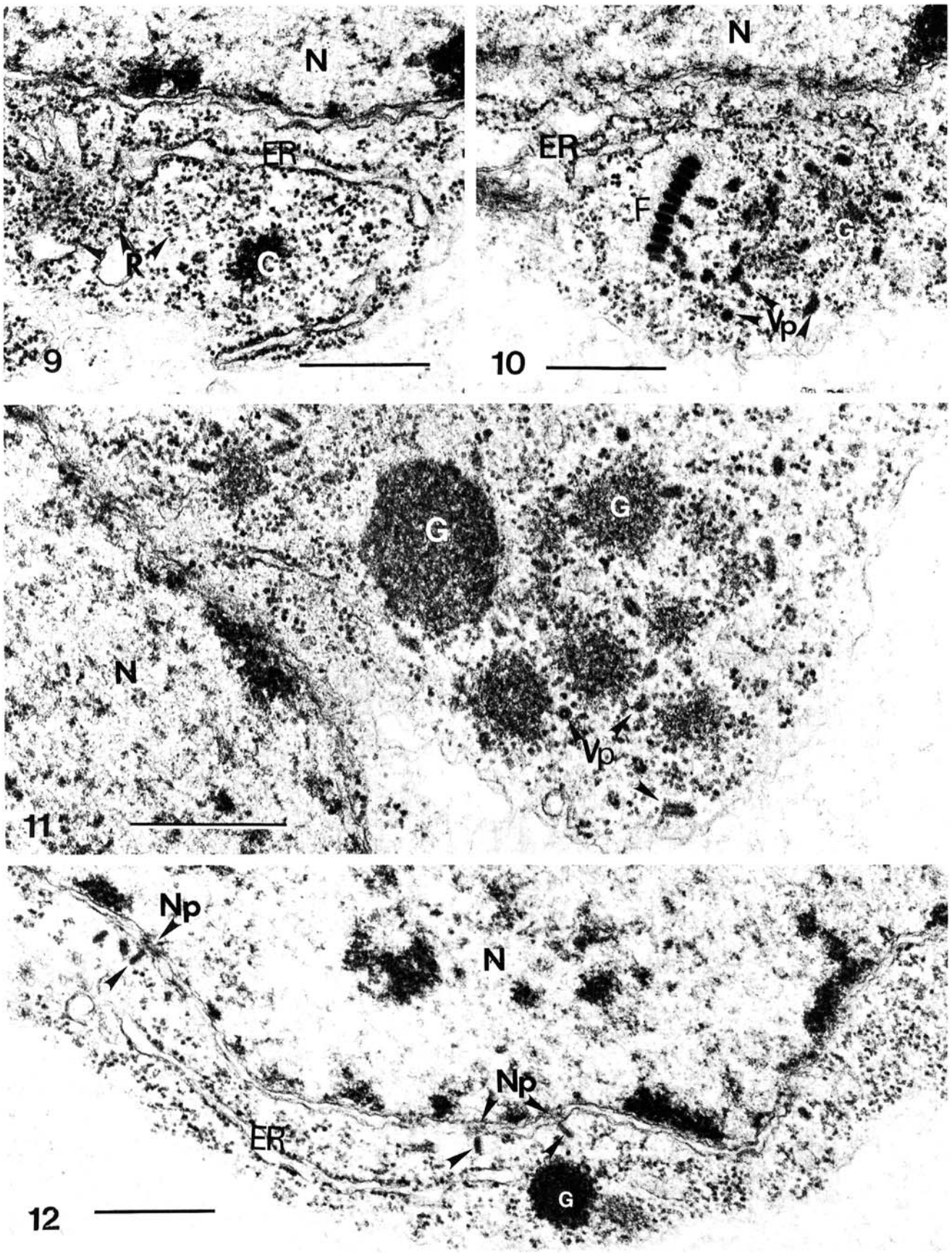

Figs. 9–12. Virus-like particles and associated inclusions found in young leaves of mimosa seedlings. **9,** Granular inclusions (G) appeared as electron-dense patches surrounded by a large number of ribosomes (R) and rough endoplasmic reticulum (ER) adjacent to the nucleus (N). Bar represents 500 nm. **10,** Virus-like particles (Vp) associated with electron-dense patches of granular inclusions (G) are randomly scattered, whereas those associated with fibrillar inclusions (F) are arranged into a "brick wall". ER = endoplasmic reticulum. Bar represents 500 nm. **11,** Several electron-dense patches of circular profiles (G) adjacent to the nucleus (N). Virus-like particles (Vp) occur randomly along the edges and between the patches. Bar represents 500 nm. **12,** Individually scattered VLPs (unlabelled arrowheads) near the nucleus, which are aligned with their short axes towards the nuclear pores (Np). G = Granular inclusion. Bar represents 500 nm.

Electron microscopy. Rod-shaped VLPs, approximately 35×95 nm, were associated with viroplasm-like inclusions in the cytoplasm of most cell types in all leaf and root specimens from mimosa trees with symptoms including approach-grafted plants and seedlings grown from seed of the infected tree (Figs. 2–4). No such particles or associated inclusions occurred in cells of any specimen taken from healthy symptomless mimosa trees.

Virus-like particles occurred only in the cytoplasm. In most cases, the VLPs occurred in an organized pattern, arranged tightly parallel to each other along their long axes (Figs. 2–4). In longitudinal sections VLPs always appeared in regularly stacked, rectangular "brick wall"-like layers (Figs. 2–4,6). When more than one layer occurred close together, they were usually aligned in the same direction appearing as multilayers of a "brick wall" (Figs. 3 and 6). In transverse sections of the particle layers, they appeared as regularly spaced paracrystalline arrays of spheres (Fig. 5). Each sphere consisted of a less electron-dense outer coat, an electron-lucent central core, and an electron-dense band between the two (Figs. 4 [inset] and 5). In some planes of sectioning the particle layers also exhibited a zigzag pattern (Figs. 2, 4, and 6).

The VLPs in fully expanded leaves were usually associated with two types of viroplasmic inclusions, fibrillar and granular, which occurred in close proximity to each other. The fibrillar inclusions appeared as conspicuous areas of cytoplasm, usually adjacent to the nucleus, consisting primarily of moderately electron-dense, homogeneous flocculent material (Figs. 2 and 4). They were usually surrounded by the rows of the VLP "brick walls" and the granular inclusions (see below) and sometimes by a number of enlarged mitochondria (Figs. 2 and 4). The granular inclusions were roughly circular bodies of various sizes consisting of a coarsely granular, electron-dense matrix (Figs. 2–4). Large granular inclusions contained one to several electron-lucent, vacuole-like areas of variable size, in which some randomly arranged VLPs were embedded (Fig. 3). The vacuoles without VLPs were filled with material similar to that of the fibrillar inclusions (Fig. 3). Individually scattered VLPs sometimes occurred along the edges of the granular inclusions, especially those granular inclusions not associated with the fibrillar inclusions (Fig. 4). Some large granular inclusions were intimately associated with many layered VLPs (Fig. 6). The particles closest to these inclusions often appeared to be formed by budding from the granular material and then aligning themselves as components of the virus aggregates in fibrillar inclusions (Fig. 6).

Abnormal cell wall protuberances, which are common in cells infected with comoviruses (9,10), nepoviruses (6,22), some caulimoviruses (2,11,13,16), and some rhabdoviruses (3), were also observed in cells containing VLPs and associated inclusions (Fig. 7). Some wall protuberances penetrated deeply into the cytoplasm, often reaching the central vacuole. In such cases, the portion of the cytoplasm accompanying the cell wall protuberance contained VLPs and associated inclusions (Fig. 7). As in the cases of some other groups of plant viruses (15,17), the VLPs of mimosa were also located near and in the plasmodesmata (Fig. 8).

Expanding leaves with typical symptoms from seedlings as young as 2 mo old contained cells that appeared to exhibit early stages of infection. For example, the granular inclusions in many of these cells appeared as small, circular electron-dense patches adjacent to the nucleus and were associated with rough endoplasmic reticulum and/or a large number of ribosomes (Fig. 9). Virus-like particles occurred randomly along the edges and between these patches (Fig. 11). Regularly arranged "brick walls" of VLPs surrounding large fibrillar inclusions, which were common features in fully grown leaves, were rarely observed in these cells. However, when a small number of the particles formed a short "brick wall", usually near the electron-dense patches of granular inclusions, they were always associated with the fibrillar inclusions (Fig. 10). Some cells in the young seedling leaves also contained individually scattered VLPs. When these particles were located adjacent to the nucleus, they were often aligned with their short axes toward the nuclear pores (Fig. 12).

Cytopathic effects in cells of root specimens from mimosa seedlings with leaf symptoms were similar to those observed in leaf cells. Virus-like particles and associated viroplasmic structures were found in many parenchymatous cells including cortical, companion, and differentiating xylem cells.

When infected tissues were fixed for Bernhard's uranyl-EDTA-lead method with Karnovsky's fixative alone, and sections were stained with 5% uranyl acetate followed by lead citrate, the cellular

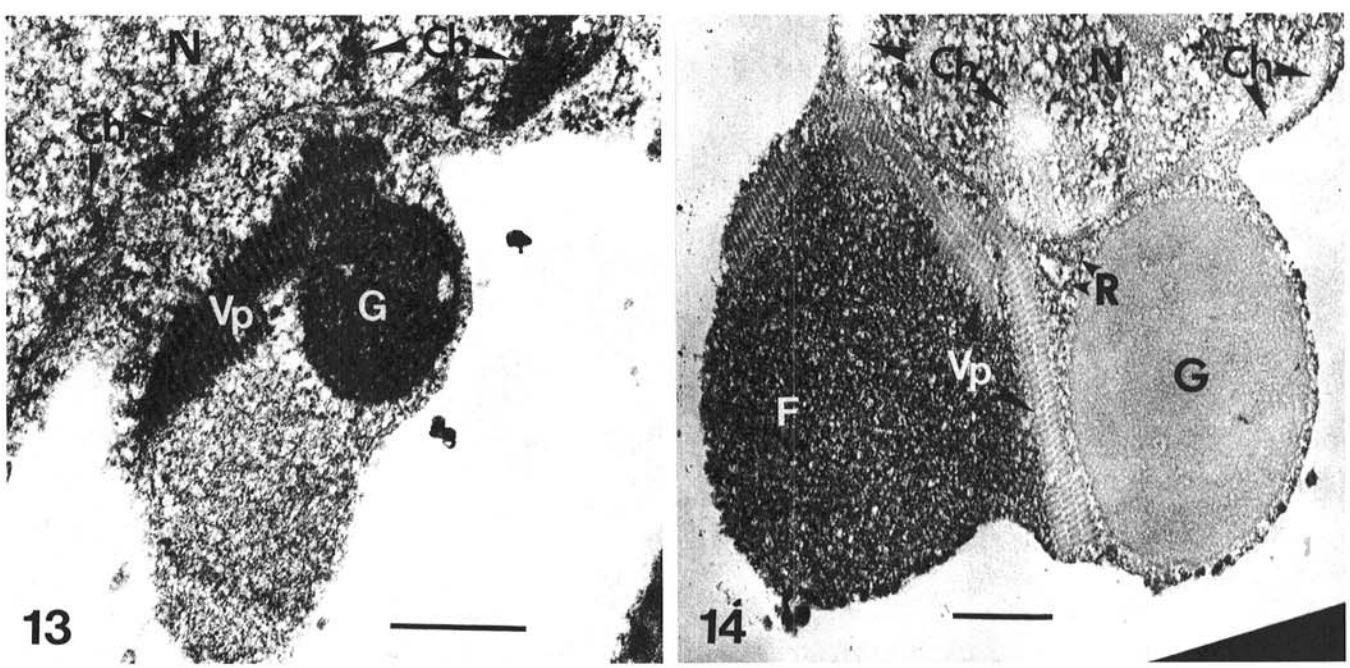

Figs. 13 and 14. The effects of Bernhard's regressive staining procedure on virus-like particles (VLPs) and associated inclusions. **13,** VLPs (Vp) and associated granular (G) and fibrillar (F) inclusions after fixation with aldehyde alone (Karnovsky's) and staining with 5% uranyl acetate and lead citrate. These structures appear similar to those prepared with aldehyde + OsO_4 fixation. Note that the VLPs, granular inclusion, and chromatin (Ch) are more electron-dense than the fibrillar inclusion. N = nucleus. Bar represents 500 nm. **14,** Similar structures to those shown in Figure 13 but after treatments with EDTA between uranyl acetate and lead citrate stains. Virus-like particles (Vp), granular inclusion (G), and chromatin (Ch) are clearly bleached, whereas fibrillar inclusion (F) and ribosomes retain their electron density. Note that the fibrillar inclusion is more electron-dense than VLPs and granular inclusion. N = nucleus. Bar represents 500 nm.

components, including crystalline arrays of VLPs and granular and fibrillar inclusions, were similar in appearance to those prepared by conventional aldehyde + OsO_4 fixation (Fig. 13). When sections were treated with EDTA for 30 min at room temperature between uranyl acetate and lead citrate stains, however, VLPs and granular inclusions as well as chromatin in the nucleus were bleached and became electron-lucent, suggesting that they are DNA-containing structures (Fig. 14). The fibrillar inclusions, on the other hand, as well as ribosomes and nucleoli, retained their electron density (Fig. 14).

A modified Bernhard's method, which involved the use of aldehyde + OsO_4 fixed tissues for distinguishing DNA- and RNA-containing structures, gave similar results. Granular inclusions, VLPs, and chromatin were all bleached, demonstrating their DNA composition, whereas fibrillar inclusions remained unchanged.

DISCUSSION

The morphology of the VLPs, the presence of viroplasmic inclusions associated with VLPs, the consistent association of these structures with the chlorotic leaf symptoms of mimosa, and the absence of these in healthy plants suggest a viral infection. In addition, the presence of abnormal cell wall protrusions and the occurrence of VLPs in the plasmodesmata, which are common cytopathic effects associated with some other plant virus groups, support this suggestion. Finally, seed- and graft-transmission of the causal agent further substantiate its viral nature.

Three described plant viruses, dendrobium virus (18), citrus leprosis virus (14), and orchid fleck virus (4), are similar in particle morphology and size to the VLPs of mimosa. Particles of all three viruses have been described as resembling the nucleocapsids of rhabdoviruses. Unlike VLPs of mimosa, however, the particles of these viruses occur primarily in the nuclei of infected cells, either associated with (4) or not associated with inclusions (14,18). In addition, the particles of these viruses form unusual "spokewheel" configurations surrounded by a membrane, which are thought to be derived from the nuclear envelope (14,18).

It is noteworthy that the granular inclusions associated with VLPs of mimosa resemble structurally the characteristic inclusions induced by caulimoviruses (17,19), a group of polyhedral viruses containing double-stranded DNA (19). In both cases, the granular inclusions contain vacuole-like areas in the matrix, and virus particles occur in the vacuoles and the outer boundary of the inclusions. Abnormal cell wall protrusions similar to those seen in infected mimosa are also common in some caulimovirus infections (2,11,13,16). These cytopathic similarities led to speculation that the particles associated with chlorosis of mimosa might be a DNA virus. Indeed, Bernhard's (1) uranyl-EDTA-lead stain technique and its alternate procedure (5) supported such speculation. Although these techniques are not conclusive, the fact that both the orderly aligned VLPs and the nearby granular inclusions, as well as nuclear chromatin, were bleached by the treatment while RNA containing nucleoli and ribosomes were not affected strongly suggests that mimosa VLPs and granular inclusions contain DNA.

Consistent association of VLPs with viroplasmic structures in the cytoplasm and the absence of such structure in the nuclei indicate that the cytoplasm is the primary site of particle production and/or assembly and that viroplasmic structures are involved in particle morphogenesis. It is of interest that two morphologically distinct types of viroplasmic inclusions occur in VLP-containing mimosa cells. Because both types usually occurred close together and were both closely associated with VLPs, it is difficult to deduce their specific function in the formation of VLPs. It is also not known which is formed first in the events of pathogenesis. Based on Bernhard's regressive staining technique, the granular inclusions contain DNA, whereas the fibrillar inclusions do not. It is, therefore, reasonable to assume that the granular inclusions are made up of precursors of viral nucleic acid and protein, and the fibrillar inclusions contain the protein alone. The association of randomly arranged particles with the granular inclusions, either at the outer edge or within the vacuolar structures of the granular inclusions, may indicate that at least some particles are formed in or from the granular inclusions and may then become organized into "brick wall" paracrystalline arrays. The particles associated with the fibrillar inclusions were always regularly arranged into the brick-wall configuration, as shown in Figures 2, 4, and 10, which suggests that the material in the fibrillar inclusions may have a role in the formation of such a particle arrangement.

LITERATURE CITED

1. Bernhard, W. 1969. A new staining procedure for electron microscopical cytology. J. Ultrastruct. Res. 27:250-265.
2. Conti, G. G., Vegetti, G., Bassi, M., and Favali, M. A. 1972. Some ultrastructural and cytochemical observations on Chinese cabbage leaves infected with cauliflower mosaic virus. Virology 47:694-700.
3. Di Franco, A., Russo, M., and Martelli, G. P. 1980. Cell wall outgrowths associated with infection by a plant rhabdovirus. J. Gen. Virol. 49:221-224.
4. Doi, J., Chang, M. U., and Yora, K. 1977. Orchid fleck virus. CMI/AAB Descriptions of Plant Viruses. No. 183.
5. Egger, D., and Bienz, K. 1975. A method for distinguishing between RNA and DNA in aldehyde and osmium tetroxide-fixed electron microscopic autoradiographs. Experientia 31:1371-1373.
6. Halk, E. L., and McGuire, J. M. 1973. Translocation of tobacco ringspot virus in soybean. Phytopathology 63:1291-1300.
7. Karnovsky, M. J. 1965. A formaldehyde-glutaraldehyde fixative of high osmolarity for use in electron microscopy. J. Cell. Biol. 27:137A.
8. Kim, K. S., Bird, J., Rodriguez, R. L., Martin, E. M., and Escudero, J. 1986. Ultrastructural studies of *Jatropha gossipifolia* infected with Jatropha mosaic virus, a whitefly-transmitted geminivirus. Phytopathology 76:80-85.
9. Kim, K. S., and Fulton, J. P. 1973. Plant virus-induced cell wall overgrowth and associated membrane elaboration. J. Ultrastruct. Res. 45:328-342.
10. Kim, K. S., and Fulton, J. P. 1975. An association of plant cell microtubules and virus particles. Virology 64:560-565.
11. Kim, K. S., Ramsdell, D. C., Gillett, J. M., and Fulton, J. P. 1981. Virions and ultrastructural changes associated with blueberry red ringspot disease. Phytopathology 71:673-678.
12. Kim, K. S., Shock, T. L., and Goodman, R. M. 1978. Infection of *Phaseolus vulgaris* by bean golden mosaic virus: Ultrastructural aspects. Virology 89:22-33.
13. Kitajima, E. W., and Lauritis, J. A. 1969. Plant virions in plasmodesmata. Virology 37:681-685.
14. Kitajima, E. W., Muller, G. W., Costa, A. S., and Yuki, W. 1972. Short, rod-like particles associated with citrus leprosis. Virology 50:254-258.
15. Kurstak, E. 1981. Handbook of Plant Virus Infection. North Holland/Elsevier, Amsterdam. 943 pp.
16. Lawson, R. H., and Hearon, S. S. 1973. Ultrastructure of carnation etched ring virus-infected *Saponaria vaccaria* and *Dianthus caryophyllus*. J. Ultrastruct. Res. 48:201-215.
17. Martelli, G. P., and Russo, M. 1977. Plant virus inclusion bodies. Adv. Virus Res. 21:175-266.
18. Petzold, H. 1971. Electron microscopic demonstration of a bacilliform virus in leaf spot diseased Dendrobia. Phytopathol. Z. 70:43-52.
19. Shepherd, R. J. 1976. DNA viruses of higher plants. Adv. Virus Res. 20:305-339.
20. Singer, I. I., and Toolan, H. 1975. Ultrastructural studies of H-1 parvovirus replication. I. Cytopathology produced in human NB epithelial cells and hamster embryo fibroblasts. Virology 65:40-54.
21. Spurr, A. R. 1969. A low-viscosity epoxy resin embedding medium for electron microscopy. J. Ultrastruct. Res. 26:31-43.
22. Yang, A. F., and Hamilton, R. I. 1974. The mechanism of seed transmission of tobacco ringspot virus in soybean. Virology 62:26-37.